

## Synchronization-induced noise reduction in spatially coupled microchip lasers

C. Serrat, M. C. Torrent, J. García-Ojalvo, and R. Vilaseca

*Departament de Física i Enginyeria Nuclear, Universitat Politècnica de Catalunya, Colom 1, E-08222 Terrassa, Spain*

(Received 15 March 2001; published 12 September 2001)

We investigate theoretically the intensity and phase correlations in the quantum-noise-driven dynamics of two spatially coupled microchip lasers. These correlations induce noise reduction phenomena for which simple analytic expressions are derived. We predict a complete suppression of the dominant relaxation oscillation peaks in the intensity difference noise spectrum, as well as photon statistics approaching the standard quantum limit. The correlations and consequent noise reduction effects are robust against frequency detuning and persist for pump powers well above threshold.

DOI: 10.1103/PhysRevA.64.041802

PACS number(s): 42.55.Ah, 42.55.Xi, 42.50.Ct, 05.45.Xt

Control of quantum noise in light sources [1] has received great attention in recent years. Advanced optical measurement technology, as high-sensitivity interferometry and spectroscopy, and optical communications, needs to circumvent the standard quantum limit (SQL) to achieve an arbitrarily desired precision. Several methods have been proposed in order to achieve the reduction of quantum noise below the SQL [2]. Specially interesting schemes are the ones reported in the frame of *twin beams*, i.e., two beams having the same intensity fluctuations, in optical parametric oscillators [3]. In that case, the suppression of quantum noise is achieved via quantum correlations in the photon pairs produced by the parametric process. In a recent paper [4], it is demonstrated that a similar kind of noise reduction may be obtained with two correlated lasers. In Ref. [4] the possibility of noise reduction is studied by considering the intensity correlation induced by correlation of the pumping mechanism. Suitable conditions are established for the difference between the correlated photodetection signals to present fluctuations below the SQL. A comparable situation might be expected from the output of spatially coupled lasers. This issue, however, has not been investigated so far. Intensity correlation in spatial coupling has only been considered in the case of unstable or chaotic lasers [5], where synchronization effects in the large-amplitude temporal variations of the system have been studied in view of their potential applications in encoded communications.

In this paper, we directly address the problem of the influence of spatial coupling on the noise properties of lasers, considering the specific case of Nd:YVO<sub>4</sub> microchip lasers working in a steady-state regime. As will be shown, strong correlations, affecting both intensity and phase, appear between the noise fluctuations induced by the spontaneous emission of each coupled laser. These correlations lead to a complete suppression of the dominant peaks in the noise spectrum of the difference between the two beam intensities and take the system near the SQL.

The system that we study consists of two laser beams of wavelength  $\lambda = 1064$  nm generated in the same crystal by two equal-intensity pump beams of wavelength  $\lambda = 808$  nm [6]. The spatial separation of the parallel pump beams may be varied and is larger than their radius, so that the population inversions of the two lasers do not overlap. The coupling between the lasers is provided by overlap of the intracavity laser fields.

In order to model our system, we have adopted a *classical* Langevin-type approach that has been successfully used by several authors, showing good agreement with experimental data in the case of solitary Nd:YVO<sub>4</sub> microchip lasers [7,8]. This approach considers the spontaneous emission factor  $\beta$  [9], and takes into account the finite decay rate of the lower laser level through nonlinear gain saturation, this last effect being a key factor in the quantum-noise properties of Nd:YVO<sub>4</sub> microchip lasers [7,8]. The evolution of the complex amplitudes of the fields  $E_j$  and the population inversions  $N_j$  is given by

$$\begin{aligned}\dot{E}_j &= -\eta E_j + g N_j E_j (1 - \epsilon |E_j|^2) + \xi E_k + i \delta_j E_j + F_j(t), \\ \dot{N}_j &= \Lambda - \gamma_{\parallel} N_j - 2g N_j (1 - \epsilon |E_j|^2) |E_j|^2,\end{aligned}\quad (1)$$

where  $j, k = 1, 2$ , with  $j \neq k$ . For simplicity, we take the same value for the cavity loss rate  $\eta$  of the two fields and consider the two lasers pumped at the same rate  $\Lambda$ .  $g = \gamma_{\parallel} \beta / 2$ , with  $\gamma_{\parallel}$  being the decay rate of the upper laser level. The nonlinear gain saturation coefficient is  $\epsilon = \gamma_{\parallel} \beta / \gamma$ , with  $\gamma$  being the decay rate of the lower laser level. The coupling coefficient is given by  $\xi = -\eta \exp[-d^2/(2r^2)]$ , where  $d$  is the separation between the fields and  $r$  is the  $1/e^2$  radius of the intensity profile [6]. In the present work, we address the case of purely dissipative coupling as a first approach to the problem, and hence the coupling coefficient  $\xi$ , which in general could be complex [10], has been taken as real.  $\delta_j$  are the laser detunings from a common reference frequency. We define the frequency detuning parameter  $\Delta = (\delta_2 - \delta_1)$ , and the normalized pump parameter  $M = \Lambda / \Lambda_{thr}$ , where  $\Lambda_{thr} \approx 2\eta/\beta$  is the threshold pumping rate of the solitary lasers. The Langevin noise sources of the fields  $F_j(t)$  are mutually *uncorrelated*, satisfying  $\langle F_j(t) F_k^*(t') \rangle = 2g N_j \delta_{jk} \delta(t - t')$ , with  $j, k = 1, 2$ .

The parameter values in our study are close to those for experiments that are feasible with Nd-based microchip lasers (see, e.g., [7,8]):  $\gamma_{\parallel} = 16.6$  ms<sup>-1</sup>;  $\beta = 1.5 \times 10^{-6}$ ;  $\gamma = 1.6$  ns<sup>-1</sup>;  $r = 220$   $\mu$ m; and  $\eta = 0.6$  ns<sup>-1</sup>. The degree of synchronization of the fluctuations in the intensities and phases of the two fields ( $E_j(t) = \sqrt{I_j(t)} \exp[i\phi_j(t)]$ ,  $j = 1, 2$ ) can be characterized by the time average of the intensity

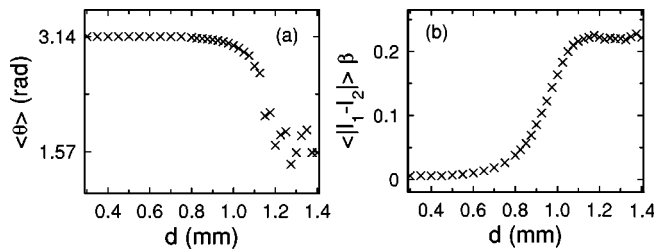


FIG. 1. Time average of the relative phase angle (a) and the intensity difference (b) between the two laser fields, as a function of the pump separation, for  $M=2$  and  $\Delta=0$ . The axes of the intensities have been rescaled with  $\beta$  along the paper.

difference  $\langle |I_1 - I_2| \rangle$ , and of the relative phase angle between the two fields, defined as  $\langle \theta \rangle \equiv \langle |\phi_1 - \phi_2| \rangle$ , with  $|\phi_1 - \phi_2| \in \{0, \pi\}$ .

As shown in Fig. 1, for a large separation  $d \geq 1.2$  mm of the pump beams within the crystal, the two lasers are *uncoupled*. The average relative phase angle between the two laser fields is  $\langle \theta \rangle = \pi/2$  rad in the uncoupled regime; the scattered behavior shown by Fig. 1(a) for  $d \geq 1.2$  mm indicates a considerable slow phase diffusion, and hence a consequent error due to the length limitation of the calculated time traces. The corresponding average intensity difference [Fig. 1(b)],  $d \geq 1.2$  mm, gives the *standard deviation* ( $\approx 0.22$  in this case) of the calculated time trace of one of the lasers. This corresponds to the expected value in an asynchronous regime.

As the value of the separation of the pump beams is decreased from  $d \approx 1.2$  mm, the laser outputs undergo a transition from the uncoupled regime to a *coupled* regime (see Fig. 1). For  $d \leq 0.9$  mm, the value of the average relative phase angle between the laser fields approaches  $\pi$  rad, as can be seen in Fig. 1(a), i.e., the two lasers become *phase-locked*. Although this phase-locking phenomenon has already been known for some time in the context of coupled lasers, our analysis of the noise dynamics of the system reveals a different insight to the phenomenon. Indeed, we find that the accuracy of phase-locking between the two lasers increases progressively as the coupling between the two lasers is increased, in such a way that, in the domain of strong coupling ( $d \approx 0.4$  mm), the locking fully affects the quantum-noise-driven fluctuations of the phases. Figures 2(a) and 2(b) show

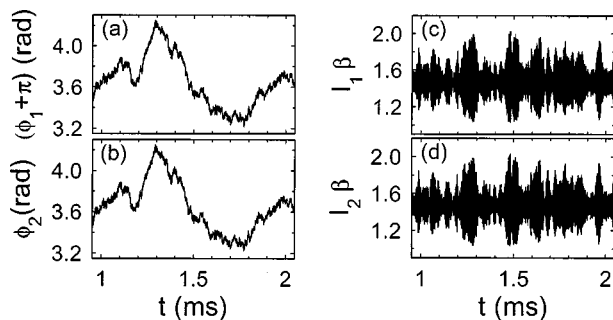


FIG. 2. Time evolution of the phases (a,b) and the intensities (c,d) of the two lasers in the strong-coupling regime ( $d=0.4$  mm), for  $M=2$  and  $\Delta=0$ .

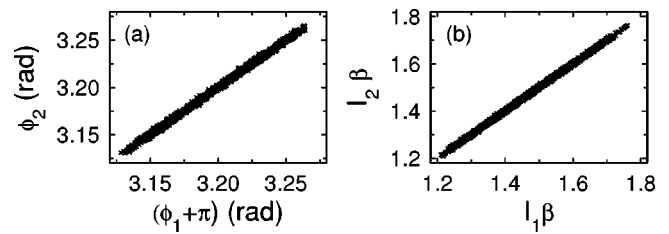


FIG. 3. X-Y plot of the time evolution of the two laser phases (a) and intensities (b), in the strong-coupling regime ( $d=0.4$  mm), for  $M=2$  and  $\Delta=0$ .

the diffusion dynamics of the phases of the two fields in the strong-coupling regime ( $d=0.4$  mm). The X-Y plot shown in Fig. 3(a) is a clear representation of this synchronized behavior. As will be discussed below, this accurate phase-locked state results in a substantial noise reduction on the relative phase of the two beams.

On the other hand, Fig. 1(b) shows that the value of the time average of the intensity difference between the two beams decreases as  $d$  is lowered, meaning that the fluctuations of the intensities of the two beams become progressively correlated. Figures 2(c) and 2(d) show the time evolutions of the intensity fluctuations of the two lasers in the strong-coupling regime ( $d=0.4$  mm). The high degree of correlation in this regime can also be observed in Fig. 3(b), where the corresponding X-Y plot is shown. The correlation in the intensities induces an important noise reduction effect in the intensity difference noise spectrum. This is the central result of this paper, and it will be further described below.

To this end, we study next the noise properties of the relative phase ( $\phi \equiv \phi_1 - \phi_2$ ) and the intensity difference ( $I_- \equiv I_1 - I_2$ ) between the two signals. To get a deeper insight, we compare computer simulations performed from Eqs. (1) with results obtained with a linearized treatment of the system [11].

The steady state ( $I_{j0}, N_{j0}, j=1,2$ ) can be derived analytically from Eqs. (1) by neglecting the noise sources  $F_j(t)$  and setting the time derivatives equal to zero. In the case of resonance ( $\Delta=0$ ), and assuming that  $I_{10}=I_{20} \equiv I_0$ ,  $N_{10}=N_{20} \equiv N_0$ , it leads to

$$N_0 = \frac{2(\eta + \xi)}{\gamma_{\parallel} \beta} \frac{I_0}{I_0(1 - \epsilon I_0) + 1}, \quad (2)$$

$$\frac{R}{1 + \beta I_0(1 - \epsilon I_0)} = \frac{I_0}{I_0(1 - \epsilon I_0) + 1}, \quad (3)$$

where  $R = \beta \Lambda / (2(\eta + \xi))$ . From Eq. (3), and using  $\beta \epsilon I_0^2 \ll \beta I_0$ , one finds

$$I_0 \approx \frac{1}{\beta} \left[ \frac{R-1}{2\zeta} + \sqrt{\left( \frac{R-1}{2\zeta} \right)^2 + \frac{\beta R}{\zeta}} \right], \quad (4)$$

where  $\zeta = (1 + \epsilon R / \beta)$ . We note that the steady-state intensity  $I_0$  increases to some extent with the absolute value of the coupling between the two fields ( $\xi < 0$ ), i.e., as the distance between the pumping beams  $d$  is reduced.

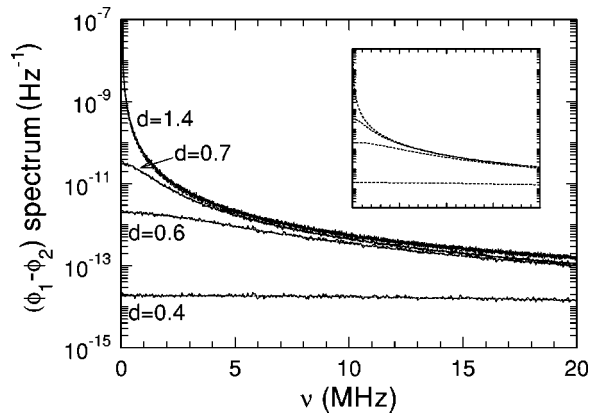


FIG. 4. Noise spectrum of the relative phase  $(\phi_1 - \phi_2)$  for  $M = 2$  and  $\Delta = 0$ , and for the indicated values of  $d$ . The dashed lines correspond to the linear theory [Eq. (5)]. Inset: curves from the linear theory alone.

The noise spectrum (frequency-dependent variance) of the relative phase  $\phi$ , in the linear approximation, results:

$$\langle \delta^2 \phi(\omega) \rangle = \frac{R_{sp}}{I_0(4\xi^2 + \omega^2)}, \quad (5)$$

where  $R_{sp} = \gamma_{\parallel} \beta N_0$ .

The effect of the degree of correlation of the phases of the two fields can be clearly observed in Fig. 4, where the noise spectrum of the phase difference between the two output fields is plotted for different values of the pump beam separation  $d$ . The results from the linearized theory [Eq. (5)] are shown in dashed lines and they have also been reproduced separately in the inset, since they largely overlap with the results from the computer simulations in the main plot. In the region of moderate coupling ( $d = 0.7$  mm), the mean relative phase of the two fields is close to  $\pi$  rad [see Fig. 1(a)], and hence the system is normally considered in this region as phase-locked. However, we observe that at this level of coupling, the time evolution of the phases is only correlated at low frequencies, and consequently the reduction of noise is only observed in the low-frequency domain. A substantial amount of noise reduction is only obtained in the region of strong coupling (Fig. 4,  $d = 0.4$  mm), in which the fluctuations of the phases become correlated in a wide frequency domain.

On the other hand, the noise spectrum of the intensity difference  $I_-$ , in the linear approximation, is given by

$$\langle \delta^2 I_-(\omega) \rangle = \frac{4R_{sp}I_0(\gamma_N^2 + \omega^2)}{(\omega_{ro}^2 + \gamma_{I_-}\gamma_N - \omega^2)^2 + 4\omega^2\gamma_{ro}^2}, \quad (6)$$

where  $\gamma_{I_-} = 2\eta - R_{sp}(1 + 2\epsilon I_0)$ ,  $\gamma_N = \gamma_{\parallel}(1 + \beta I_0)$ ,  $\omega_{ro} = \gamma_{\parallel}\beta R_{sp}I_0$ , and  $\gamma_{ro} = (\gamma_{I_-} + \gamma_N)/2$ .

Lines (1), (2), and (4) in Fig. 5 show the normalized intensity difference noise spectrum calculated for  $M = 2$  and  $\Delta = 0$ :  $d = 1.4$  (line 1),  $d = 0.75$  (line 2), and  $d = 0.6$  (line 4). The results from the linearized theory [Eq. (6)] describe most of the features of the complete nonlinear system. The only

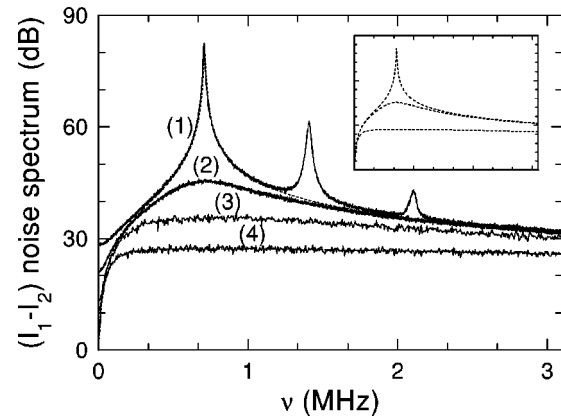


FIG. 5.  $(I_1 - I_2)$  noise spectrum normalized to the SQL, for  $M = 2$ . The dashed lines correspond to the linear theory [Eq. (6)]. (1)  $d = 1.4$ ,  $\Delta = 0$ ; (2)  $d = 0.75$ ,  $\Delta = 0$ ; (3)  $d = 0.6$ ,  $\Delta = 1.85\xi$ ; (4)  $d = 0.6$ ,  $\Delta = 0$ . Inset: curves (1), (2), and (4) from the linear theory alone.

discrepancies arise at the low-frequency wing of the spectrum, where the numerical calculations have a limited precision, and at the harmonics of the relaxation oscillations frequency, where the peaks are absent because of their intrinsic nonlinear origin. Clearly, increasing the coupling between the laser fields rapidly reduces the dominant relaxation oscillations peak and suppresses its harmonics (line 2), and at still moderate coupling,  $d = 0.6$  mm (line 4), all the peaks disappear. Line (3) in Fig. 5 corresponds to  $d = 0.6$  mm and to cavity detuning  $\Delta = 1.85\xi$  ( $\Delta \approx 27\mu s^{-1}$ ) and shows the robustness of the synchronization (and of the consequent noise reduction effect) against frequency detuning.

We study the photon statistics of the intensity difference  $I_-$  by measuring the Fano factor [7,12], which is defined as the variance of  $I_-$  normalized with respect to the SQL ( $2I_0$ ). Its expression is obtained from the linear approximation by integrating Eq. (6) over all frequencies, yielding

$$F \equiv \frac{\langle \delta^2 I_- \rangle}{2I_0} = \frac{R_{sp}}{2\gamma_{ro}}. \quad (7)$$

Figure 6 shows the behavior of the Fano factor as a function of the pump separation. The Fano factor is a representation of the statistical *second moment* (variance) of the fluctuations in  $I_-$ , and can be compared with Fig. 1, which represents the *first moment* (mean). Calculations are shown in Fig. 6 for two different values of the pump parameter  $M = 2, 50$ . Again, the results from the linearized theory [Eq. (7)] are in excellent agreement with the numerical simulations. Clearly, the Fano factor progressively decreases with increasing coupling, though it remains always above unity; for strong coupling ( $d \approx 0.4$ ) the Fano factor approaches unity, meaning that the photon statistics of the intensity difference ( $I_-$ ) approaches a Poissonian distribution. Figure 6 includes two numerical simulations calculated with frequency detuning ( $\Delta = \xi$ ). The effect of detuning is relatively weak in the behavior of the Fano factor. The first effects of frequency detuning are observed for  $\Delta > \xi/10$ , and they are more important for higher values of the pump parameter, as can be

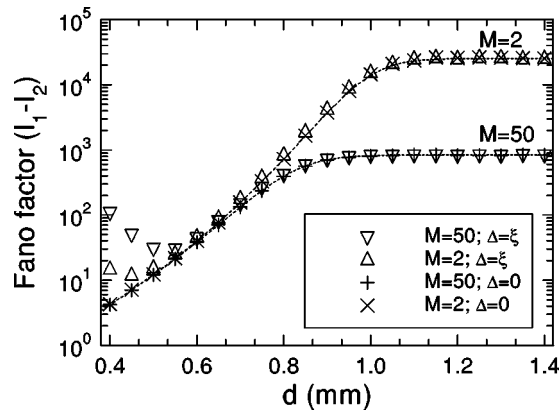


FIG. 6. Fano factor corresponding to the intensity difference signal ( $I_1 - I_2$ ) as a function of the pump beam separation  $d$ . The dashed lines correspond to the linear theory [Eq. (7)].

observed in Fig. 6. Note that the detuning  $\Delta$  is included in the calculations of Fig. 6 as a function of the coupling itself ( $\Delta = \xi$ ); this leads, e.g., to a value of the frequency detuning such as  $\Delta \approx 0.1 \text{ ns}^{-1}$  for a pump separation such as  $d = 0.4$ . Finally, we have also performed calculations for higher values of the pump power, and we can assert that the synchronization remains substantially accurate for  $\Lambda/\Lambda_{thr} < 200$ , at least.

As a conclusion, we have shown that the intensity and phase fluctuations driven by spontaneous emission in two spatially coupled Nd:YVO<sub>4</sub> microchip lasers working in a steady-state regime become highly correlated when the lasers are strongly coupled. The phase and intensity correlations

occur because they maximize the gain of the system, as can be shown by further developing Eqs. (1) [11]. The key point here is that this synchronization applies not only to large amplitude fluctuations, such as those observed, e.g., in unstable coupled lasers [5], but also to the dynamics of the small fluctuations that we have considered, which are continuously fed by quantum noise, and this can be used to induce noise reduction effects in the system.

Interestingly, our study provides a characterization of the degree of accuracy of the phase-locking phenomena observed in spatially coupled lasers. The study of the noise reduction in the spectrum of the difference between the two beam intensities as a function of the coupling strength exhibits a complete suppression of the dominant relaxation oscillations peak and of its harmonics at a moderate coupling, although the photon statistics remains always above the SQL.

It is likely that the effects presented here can be observed in many different types of spatially coupled lasers whose solitary dynamics are usually described by rate equations. It will also be interesting to study the noise characteristics of the sum of the synchronized output fields studied here, and this will be published elsewhere.

We would like to thank M. P. van Exter for helpful discussions on the spatial coupling coefficient. We are grateful to R. Roy and M. San Miguel for their comments on the subject. This research was supported by DGESIC (Spain) (Project No. PB98-0935-C03-01), the Generalitat of Catalunya (Project No. 1999SGR00147), and CESCA/CEPBA.

- 
- [1] L. Davidovich, *Rev. Mod. Phys.* **68**, 127 (1996).  
 [2] *Squeezed Light*, edited by R. Loudon and P.L. Knight, special issue of *J. Mod. Opt.* **34**, 703 (1987).  
 [3] A. Heidmann, R.J. Horowicz, S. Reynaud, E. Giacobino, and C. Fabre, *Phys. Rev. Lett.* **59**, 2555 (1987).  
 [4] A.Z. Khoury, *Phys. Rev. A* **60**, 1610 (1999).  
 [5] R. Roy and K.S. Thornburg, *Phys. Rev. Lett.* **72**, 2009 (1994); M. Möller, B. Forsmann, and W. Lange, *Quantum Semiclass. Opt.* **10**, 839 (1998); R. Kuske and T. Erneux, *Opt. Commun.* **139**, 125 (1997); J. García-Ojalvo, J. Casademont, M.C. Torrent, C.R. Mirasso, and J.M. Sancho, *Int. J. Bifurcation Chaos Appl. Sci. Eng.* **9**, 2225 (1999).  
 [6] L. Fabiny, P. Colet, R. Roy, and D. Lenstra, *Phys. Rev. A* **47**, 4287 (1993).  
 [7] N.J. van Druten, Y. Lien, C. Serrat, S.S.R. Oemrawsingh, M.P. van Exter, and J.P. Woerdman, *Phys. Rev. A* **62**, 53808 (2000).  
 [8] C. Becher and K.J. Boller, *J. Opt. Soc. Am. B* **16**, 286 (1999).  
 [9] See, for instance, M.P. van Exter, G. Nienhuis, and J.P. Woerdman, *Phys. Rev. A* **54**, 3553 (1996), and references therein.  
 [10] G. Bouwmans, B. Segard, D. Dangoisse, and P. Glorieux, *J. Opt. Soc. Am. B* **17**, 781 (2000).  
 [11] Further details on the theory presented here will be given in a separate paper.  
 [12] P.R. Rice and H.J. Carmichael, *Phys. Rev. A* **50**, 4318 (1994).